TILT ROTOR AEROMECHANICS PHENOMENA IN LOW SPEED FLIGHT

Mark A. Potsdam
Aerospace Engineer, Aeroflightdynamics Directorate
U.S. Army Aviation and Missile Research, Development, and Engineering Center
Moffett Field, CA
mpotsdam@mail.arc.nasa.gov

David F. Schaller
Lead Engineer, Sukra Helitek
Ames, IA
dfs2@sukrahelitek.com

R. Ganesh Rajagopalan
Professor, Department of Aerospace Engineering
Iowa State University
Ames, IA
rajagopa@iastate.edu

Mark J. Silva
Aerospace Engineer, Advanced Aerodynamics Branch
U.S. Navy NAVAIR Air Vehicle Department
Patuxent River, MD
mark.silva@navy.mil

ABSTRACT

This work investigates important aeromechanics phenomena affecting the V-22 tilt rotor in low speed sideward flight or while hovering in quartering or crosswind conditions. These phenomena, such as pitch-up with sideslip and increased power required in sideward flight, were identified during V-22 critical azimuth flight testing and impacted handling qualities in this flight regime. Navier-Stokes computational fluid dynamics (CFD) calculations with varying degrees of modeling fidelity are presented and compared with flight test data. In general, CFD predicts the flight test trends as a function of wind speed and direction in agreement with data. Detailed investigation clearly shows the interaction of the rotor wake with the airframe as the major cause of the aeromechanics phenomena seen on the V-22. Identification of the underlying flowfield physics allows investigation of options for alleviation and prediction of future tilt rotor configurations.

NOTATION

C_M pitching moment coefficient, $M_Y / \rho(\Omega R)^2 \, 2\pi R^3$
C_Q rotor torque coefficient, $Q / \rho(\Omega R)^2 \, \pi R^3$
C_T rotor thrust coefficient, $T / \rho(\Omega R)^2 \, \pi R^2$
DL/T   airframe download divided by total thrust
M_{tip} hover tip Mach number
PUWSS   pitch-up with sideslip
R   rotor radius
TPP tilt   equivalent tip path plane tilt, $\sin^{-1}(C_M R / C_T \Delta z)$
v_0 hover induced velocity, $v_{tip}\sqrt{C_T/2}$
β wind azimuth, degrees
Δz vertical distance between CG and rotor hub
θ blade collective angle at r/R = 0.75, 14 degrees
ρ air density
Ω rotor rotational speed

INTRODUCTION

Tilt rotor aircraft are recognized for their ability to significantly change both the military and civilian aviation transportation landscapes. The range and speed of a turboprop airplane is augmented by the ability to operate in and out of confined areas like a helicopter. For civilian operations this means reduced impact on an already overloaded airspace system and reduced infrastructure costs. For military operations, increased payload and range with reduced aerial refueling operations are possible when compared with helicopters currently performing the same remote area missions. Taking advantage of the helicopter mode capability allows tilt rotors to hover in place, maneuver around an airfield at low speed, and conduct shipboard operations with wind over the deck. The V-22 Osprey is the first production military tilt rotor aircraft.

The objective of this work is to investigate important aeromechanics phenomena affecting the V-22 tilt rotor in operations requiring low speed flight in any direction or hovering in wind conditions. The two maneuvers are

aerodynamically equivalent and will be used interchangeably. During V-22 critical azimuth flight testing designed to evaluate control margins and pilot workload under such flight conditions, phenomena such as pitch-up with sideslip (PUWSS) and increased power required in sideward flight were identified [1]. These phenomena adversely impacted handling qualities in this flight regime. Modifications to the flight control system were required in order to restore full control authority without reaching control limits in multi-axis maneuvers. Also identified was a sharp drop in power required in forward and rearward flight when passing though 25 knots.

However, there has been limited exploration to identify the detailed aerodynamic interactions involved [2]. As revealed by computational fluid dynamics (CFD), the cause of these phenomena is the interaction of the rotor wakes with the airframe. These interactions are somewhat specific to the V-22 configuration, having not been seen, or perhaps recognized, on earlier tests of the XV-15 [3]. Nonetheless, it is important to appreciate these phenomena when present in the operation of tilt rotors so that revisions can be made to standard operating procedures and flight operations manuals. The design of future tilt rotors should also consider these interactions, with further research required on aircraft geometric characteristics that trigger the phenomena. Such aerodynamic interactions are likely to play an important role in the ability of runway independent aircraft to fit into the national airspace system and effectively maneuver around an airfield to their best advantage.

In addition to the available V-22 flight test data, several experimental efforts have investigated rotor/airframe interactions on tilt rotor aircraft. The majority of this work focused on no-wind hover. However, it is likely that hover in winds from varying azimuths is a more common flight condition. McVeigh [4] investigated both no-wind and headwind hover conditions with no side winds. XV-15 flight testing [3] was performed for no-wind hover, sideward, and rearward flight.

Previous computational work by the authors has shown that CFD can accurately predict both isolated tilt rotor performance and airframe loads for tilt rotor configurations in no-wind hover [5,6]. Tilt rotor CFD computations by other investigators have mainly been limited to no-wind hover, predicting tilt rotor download [7,8]. The present work extends earlier research to side wind conditions.

V-22 CONFIGURATION

A computational model has been constructed of a V-22 airframe configuration in hover. The fuselage is the Full-Scale Development (FSD) configuration generated using high-fidelity V-22 fuselage, wing, nacelles, and tail geometry. The FSD differs from the Engineering, Manufacturing & Development (EMD) fuselage used in flight testing in that the fuselage strakes are absent, the aft part of the sponsons are recontoured, and minor antenna and excrescence differences exist. The wing flaperon angle is set to 67 degrees in the CFD model, while flight test data were taken with a 72.5 degree setting. The difference in flaperon setting may change the download by up to 4% [9]. The effects of other geometric differences on critical azimuth test conditions are expected to be minor.

The rotor blade geometry is a representation of the NASA Tilt Rotor Aeroacoustics Model (TRAM) rotor [10]. The TRAM is an extensive wind tunnel model constructed to facilitate future tilt rotor aeromechanics research. The rotor geometry is a 0.25-scale 3-bladed V-22 rotor with geometric and dynamic scaling. The only geometric differences are in the blade cuff region inboard of 25% blade radius.

CRITICAL AZIMUTH TESTING

As part of the overall V-22 Osprey EMD Program, handling qualities flight testing was performed to demonstrate, among other things, critical azimuth capabilities of the tilt rotor [1]. Initial tests were conducted at sea level (Patuxent River, MD) followed by high density altitude testing (Fort Huachuca, AZ) at ~7000 ft. In both cases, light and heavy gross weight conditions were demonstrated. Most conditions were flown using a pace vehicle. Real time local wind measurements (speed and direction) were recorded. Handling quality trends were deemed independent of density altitude. The V-22 was demonstrated in winds around the full 360º azimuth and speeds up to the 45 knots required by design specifications. The V-22 in critical azimuth testing is shown in Figure 1.

Several differences in attitude and flight control positions occur due to operational procedures in flight testing which are difficult to duplicate in a computational model. In critical azimuth flight testing the V-22 fuselage, nacelles, and rotors are controlled to maintain aircraft trim. In order to maintain balance, the pitch attitude of the

Figure 1 V-22 in critical azimuth flight testing.

fuselage naturally varies between –3 and +10 degrees and the roll attitude varies between ±10 degrees throughout the wind azimuth envelope. Power is controlled to set rotor thrust in order to balance weight, download, and jet thrust. Control of the rotors through collective and lateral and longitudinal cyclic is used to maintain trim in side flight conditions. Longitudinal cyclic controls pitch, differential longitudinal cyclic controls yaw, and differential collective controls roll. Additionally, the gimbaled hub allows the rotor to flap. When approaching forward longitudinal stick limits, the nacelles are programmed to automatically transition forward to 85 degrees. This creates a pitching moment and restores full authority to the flight control system. Aircraft center of gravity (CG) was varied during testing.

In the CFD calculations the fuselage pitch and roll attitudes are maintained at zero. The collective angle, θ, is fixed at 14 degrees; therefore, the solutions are not trimmed to a constant thrust or weight. In spite of this, the total rotor thrust is relatively constant ($C_T \approx .015 \pm 4\%$). Two hover tip Mach numbers (M_{tip}) were investigated. Maximum interim (continuous) power at sea level corresponds to a value of $M_{tip} = 0.736$ (104% Nr). A lower value of 0.625 (88% Nr) was also investigated corresponding to TRAM experiments. The rotor parameters $M_{tip} = 0.736$ and $\theta = 14$ degrees correspond to a V-22 medium gross weight at a high density altitude or a high gross weight at sea level. No rotor control cyclic inputs were specified and rotor flapping is not allowed. The nacelle angles are maintained at 90 degrees. In the CFD moment calculations, the center of gravity is at a nominal location for hover. No attempt was made to trim the aircraft in the various flight conditions.

It can be expected that some of these geometric and operational differences will affect the absolute levels of the airframe and rotor parameters. For example, it has been shown that fuselage pitch angle shifts the download versus headwind speed curve and modifies its shape slightly [4].

METHODOLOGY

Two complementary CFD methodologies are applied to the V-22 configuration in sideward flight. Both solve the unsteady Navier-Stokes equations, but with varying degrees of modeling accuracy. The two codes offer the obvious trade-offs between fidelity and speed, with known advantages, disadvantages, and limitations.

OVERFLOW-D

A subset of CFD calculations use the Reynolds-averaged Navier-Stokes code OVERFLOW-D [11]. It is based on the OVERFLOW 1.6au code, which has been continually developed at NASA and has been applied to a wide range of fluid dynamics problems. OVERFLOW-D

includes major modifications for time-dependent, rigid body motion of components, in particular individual moving rotor blades. Solutions are computed on structured, overset grids using body-conforming "near-body" grids and automatically generated Cartesian "off-body" grids in the wake and farfield.

For spatial discretization, OVERFLOW-D uses 4th-order central differencing with artificial dissipation. The time-accurate analysis uses an implicit 1st-order algorithm in the near-body grids and an explicit 3rd-order Runge-Kutta scheme in the off-body grids. The Baldwin-Barth one-equation turbulence model is used in the near-body grids, which are assumed fully turbulent. Off-body grids are modeled as inviscid in order to reduce the numerical dissipation in the wake.

In the Chimera methodology, overset, structured near-body grids are generated about the geometry. The complete configuration, including the rotors, fuselage, and nacelles, is modeled as viscous. The near-body grids have sufficient resolution and extent to capture wall-bounded viscous effects. High resolution C-mesh topology blade grids are used. The V-22 surface grids are shown in Figure 2. For the moving rotors, the nacelle spinner rotates with the blades.

Off-body Cartesian grid generation is automatically performed by OVERFLOW-D. The finest off-body spacing is 10% of the rotor tip chord. This level-1 off-body grid surrounds the rotors and the fuselage and captures the wake. Progressively coarser levels are generated out to the farfield boundary at 6.5 rotor radii from the center of the domain. Freestream characteristic conditions are applied to the farfield outer boundary. Where grid points fall inside the geometry, hole cutting is employed to blank out these points. A streamwise cross-sectional cut through the volume grid system in Figure 3 shows the near- and off-body grids, hole cuts, and overlap for half the V-22 configuration. The total number of grid points in the full-span V-22 model is 47.6 million with 63% in the off-body grids. More details can be found in Reference 5.

Solutions are computed on large parallel computers or a network of PCs/workstations communicating with the
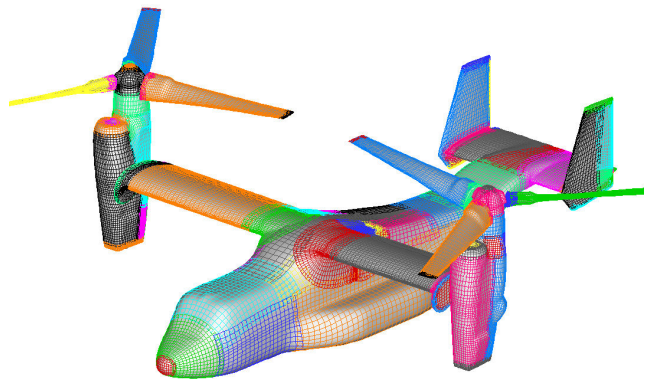

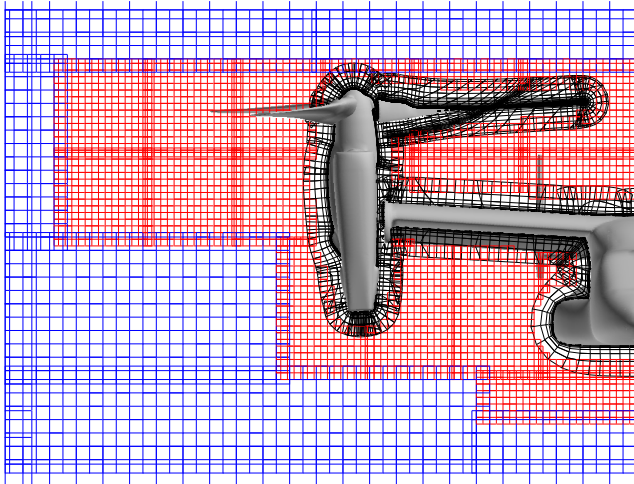**Figure 2 OVERFLOW-D V-22 surface grids.**

Figure 3 Slice through OVERFLOW-D volume grids (every third point). black – near-body, red – finest level off-body, blue – coarser level off-body.

Message Passing Interface (MPI) protocol. Both the domain connectivity and flow solver modules have been parallelized for efficient, scalable computations using MPI. OVERFLOW-D simulations were run on 128 processors of either an IBM Power3 (375MHz) or Power4 (1.3 GHz) supercomputer. Each rotor revolution requires 5 wallclock hours for 2400 iterations per revolution on the Power4. Domain connectivity accounts for 20% of the wallclock time. Solutions run on the Power3 require 11 hours per rotor revolution: 2.2X slower.

Rot3DC

Rot3DC was used to simulate a more complete matrix of cases. Rot3DC is a CFD code developed by Sukra Helitek, Inc. and specializes in rotor applications [12]. The rotor is modeled using a momentum source technique developed by Rajagopalan [13]. Rot3DC solves the incompressible, Reynolds-averaged Navier-Stokes equations for the computational domain with the rotor momentum added as time-averaged source terms. The rotor disk momentum jumps are determined by two-dimensional airfoil table lookup and then time-averaged around the azimuth. The wake system continually feeds back into the rotor inflow characteristics. The SIMPLER algorithm [14] is used to solve the discretized Navier-Stokes equations. No turbulence model was employed during the current simulations.

Rot3DC uses a structured Cartesian grid to model the entire computational domain. A body is represented by a blocked grid cell method. Cells which are marked as body cells have a no-slip, no-penetration condition applied to them. The Cartesian grid is simple to generate, but the mesh must be very fine near the body to achieve a reasonable level of fidelity. The structured mesh has 152x129x121
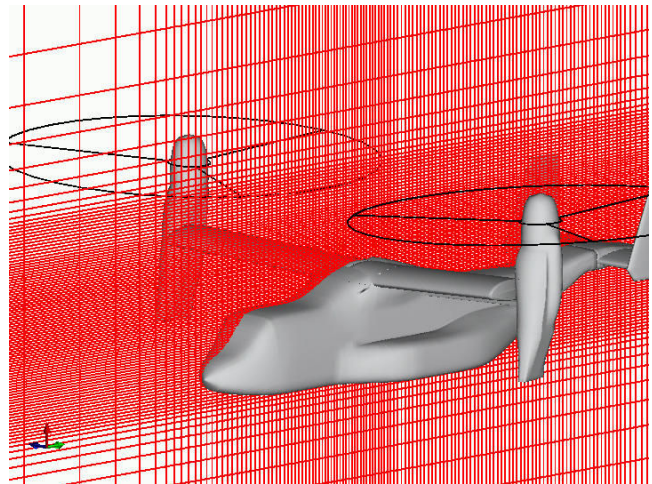

Figure 4 Slice through Rot3DC volume grid.

cells in the streamwise, spanwise, and normal directions, respectively. Of the 2.37 million grid cells, 2.3% (54,000) are body cells. The mesh extends about 20 rotor diameters from the aircraft CG in all directions. Freestream conditions are specified at the far field inlet boundaries. The volume grid is shown in Figure 4.

Rot3DC simulations were run on individual single processor PC-class machines. The speed of the processors used ranged from 700 MHz to 3.0 GHz. On a 2.4 GHz machine, each equivalent rotor revolution requires 8.5 wallclock hours for 426 iterations.

CODE COMPARISON

OVERFLOW-D has the advantage of high geometric and physical modeling fidelity with time-dependent moving blades, wall bounded turbulent viscous layers, and exacting grid resolution. These come at the expense of considerable effort and expertise for grid generation and problem setup. Computational cost on large-scale parallel supercomputers is prohibitive for engineering analyses. Rot3DC requires minimal user setup, and grid generation is automated. Computational cost is moderate on inexpensive single processor desktop PCs. The trade-off is a lower level of geometric and physical modeling. Additionally, wall bounded flows are not accurately captured without body conforming grids, viscous grid spacing, and a turbulence model. In cases where the detailed flow about the rotors is less important or important only on a time-averaged basis, actuator disk modeling is often sufficient [12].

In this work, Rot3DC has been used to advantage to run a fine matrix of test cases, varying wind speed and direction. Apparent trends are investigated. OVERFLOW-D has been used to compute a subset of conditions with a thorough investigation of the flow physics mainly via flowfield visualization.

AEROMECHANICS PHENOMENA

During V-22 critical azimuth testing, several aeromechanics phenomena were identified that adversely affected handling qualities. Independently, the phenomena have been recognized in CFD calculations. CFD has been particularly useful in detailing the causes of the phenomena. In this work the following aeromechanics phenomena will be specifically addressed:

− Pitch-up with side slip (PUWSS)
− Increasing power in sideward flight
− Forward/rearward flight

They will be discussed in the context of:

− Airframe download/thrust (DL/T) and equivalent tip path plane (TPP) tilt
− Breakdown of airframe forces/moments by aircraft component (wing, fuselage, nacelle, sponsons, tail)
− Isolated fuselage characteristics
− Trends with wind speed and azimuth
− Trends with rotor tip speed
− Rotor performance and rotor-on-rotor effects

Figure 5 from V-22 critical azimuth flight testing [1] details the trends of several flight control parameters as a function of wind speed and direction. Figure 6, also from Reference 1, shows the power required in head and tailwinds as a function of wind speed.

ANALYSIS AND DISCUSSION

All CFD solutions were run at a fixed 14 degrees collective ($C_T \approx 0.015$), 0.25-scale V-22 (TRAM) Reynolds number, 90° nacelle tilt, zero fuselage pitch angle, and no trim considerations.

The Rot3DC matrix of runs includes wind speeds ranging from 15 to 45 knots in 10-knot increments with wind azimuths of 0, 45, 90, 135 and 180 degrees. In addition, at 15 and 35 knots, wind azimuths of 30 and 60 degrees have been simulated. The tip Mach number was fixed at 0.625. Each run completes just over 14 equivalent rotor revolutions. The results are time averaged for the last seven revolutions. Rot3DC uses a table look-up method for the rotor airfoil properties, so a low Reynolds number airfoil table was used to model the blades. This low airfoil table has proven to be very accurate for past modeling of the TRAM rotors.

OVERFLOW-D simulations were run for 0, 45, 90, 135, and 180 degrees wind azimuth at a 35-knot wind speed and 15 to 35 knots in 5-knot increments at 0 degrees azimuth. Two hover tip Mach numbers (0.625 and 0.736) were investigated, as well as cases with rotors not turning. The baseline condition for OVERFLOW-D is $M_{tip} = 0.736$ unless specified. Calculations with winds were initiated from hover or nearby wind conditions. In general 10 to 15 rotor revolutions are required to remove transients when
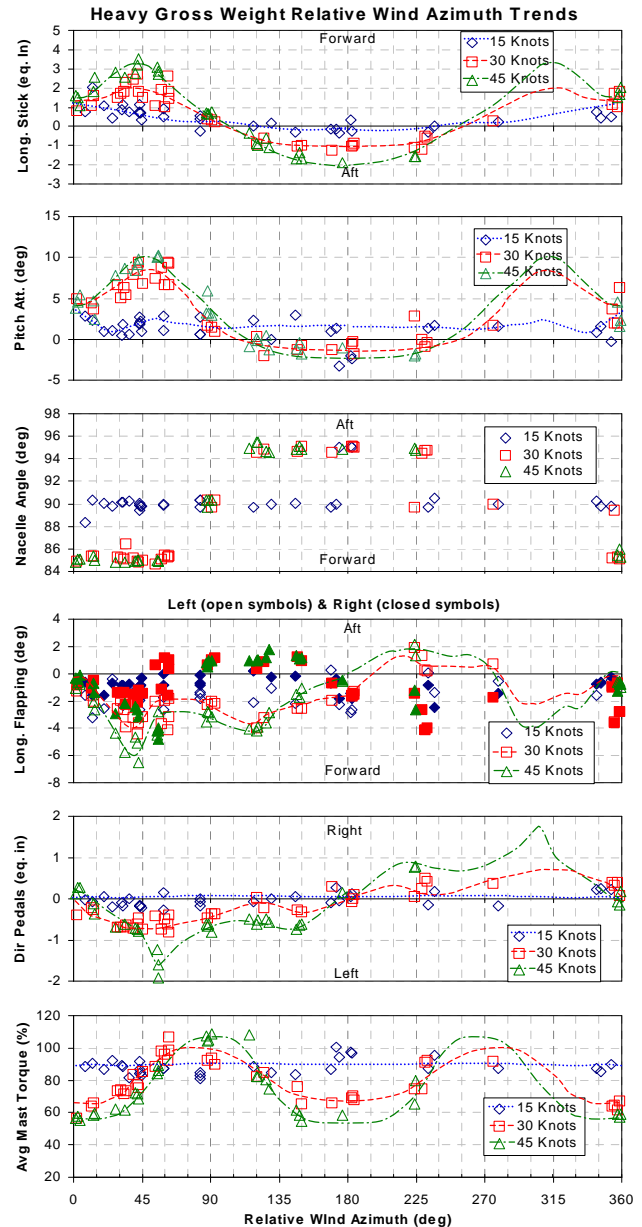

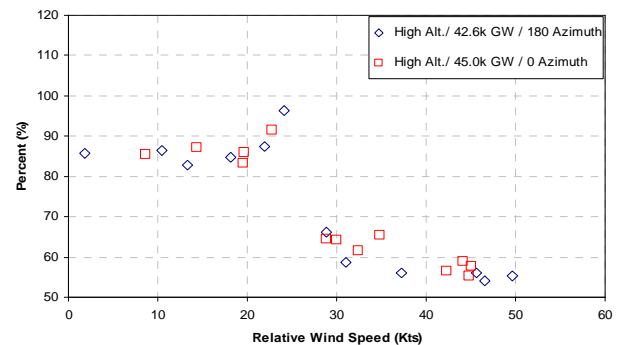**Figure 5 V-22 critical azimuth flight test data [1].**

Figure 6 V-22 flight test average mast torque (%) for head and tailwinds [1].

parameters such as wind speed or direction are changed. All time-averaged results are averages over at least 5 rotor revolutions. Sample time histories of rotor performance and airframe forces are shown in Figures 7 and 8, respectively, for a 35-knot wind speed as a function of wind azimuth. Some conditions are steadier and would therefore have improved handling qualities. Major oscillations are 3 per rotor revolution due to the 3-bladed rotors.

Pitch-up with Sideslip

PUWSS is a well-understood aeromechanics phenomenon in which the upwind rotor wake impinges on the horizontal tail causing the aircraft to pitch up [1,2]. The phenomenon is most critical with wind from ±45° azimuths, although it is seen in a range from 30 to 70 degrees. The

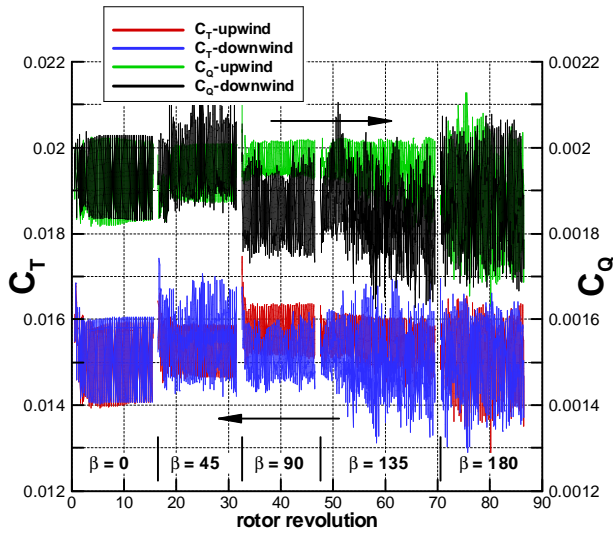pitching moment generated must be counteracted. The significant longitudinal stick displacement (longitudinal flapping), increased fuselage pitch attitude, and 85° nacelle tilt required are evident in the flight test data (Figure 5) for quartering headwinds with speeds greater than 20 knots. The V-22 flight control system is programmed to tilt the nacelles forward 5 degrees automatically when longitudinal cyclic and flapping limits are approached in this condition. PUWSS was not documented for the XV-15.

In the CFD calculations, PUWSS is noted as an increase in airframe pitching moment, C_M, equilibrated to a TPP tilt (longitudinal flapping) required to counteract the moment. Equivalent TPP tilt is shown schematically in Figure 9 and determined from the following equation:

$$\text{TPP tilt} = \sin^{-1}\left(C_M R / C_T \Delta z\right)$$

Positive tip path plane tilt (flap down in front) counteracts a nose up pitching moment.

Rot3DC time-averaged DL/T and equivalent TPP tilt are shown in Figure 10 as a function of wind direction and

Figure 7   OVERFLOW-D rotor performance time histories as a function of wind azimuth, 35-knot wind.
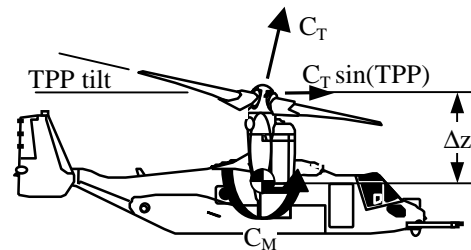
Figure 9 Definition of equivalent tip path plane (TPP) tilt.

Figure 8   OVERFLOW-D airframe coefficient time histories as a function of wind azimuth, 35-knot wind.

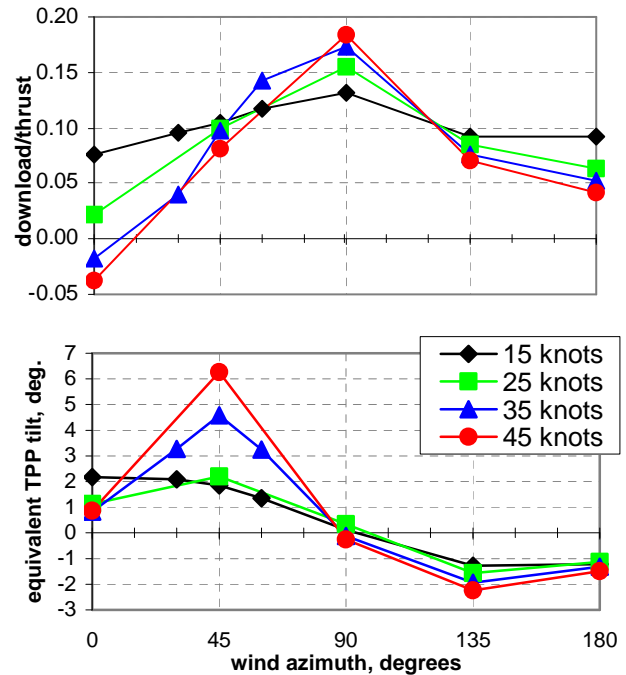**Figure 10   Rot3DC time-averaged airframe DL/T and equivalent TPP tilt as a function of wind speed.**

Figure 12 OVERFLOW-D time-dependent particle traces. Particles released from upwind (left) blade tips impinge on tail, 35 knot wind at 45° azimuth (→), $M_{tip} = 0.625$.
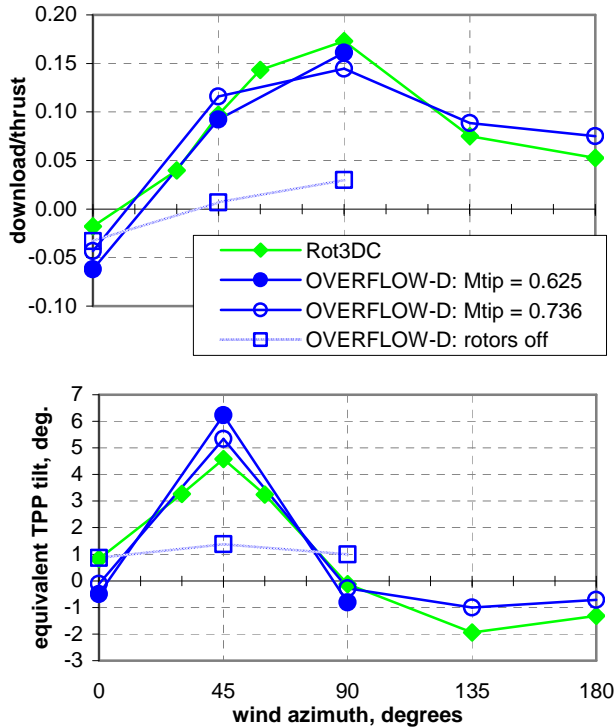

Figure 11 Comparison of OVERFLOW-D and Rot3DC time-averaged airframe DL/T and equivalent TPP tilt, 35-knot wind.

Figure 13 OVERFLOW-D time-averaged airframe DL/T and equivalent TPP tilt by airframe component, 35-knot wind.

speed. OVERFLOW-D time-averaged values are shown in Figure 11 for a 35-knot wind speed, with and without rotors. Note that the pitch-up is not indicated in the fuselage-only OVERFLOW-D calculations, where the rotor motion has been turned off, indicating that this is an adverse rotor-airframe interaction. Calculated pitch-up trends are in excellent agreement with flight test measurements. All show maximum pitch-up at the 45° wind azimuth with symmetric behavior about this azimuth. Rot3DC calculations correctly predict pronounced pitch-up characteristics for wind speeds greater than 25 knots with increased severity as wind speed increases. Outside the PUWSS region, in tailwind conditions with the wind azimuth greater than 90°, CFD predicts pitch-down characteristics. This correlates with the aft longitudinal stick, negative fuselage pitch attitude, and 95° nacelle tilt in flight test.

OVERFLOW-D and Rot3DC results are directly compared in Figure 11. Download is in excellent agreement for these conditions, except for a disagreement in the headwind condition. OVERFLOW-D predicts more severe pitch-up than Rot3DC, by 1.7° TPP tilt, at the critical 45° azimuth. The maximum pitching moment is increased by 17% as the hover tip Mach number is increased from 0.625 to 0.736 in OVERFLOW-D. However, the equivalent TPP tilt is reduced by 14% for the higher tip Mach number. A minimum in TPP tilt occurs at a quartering 135° tailwind
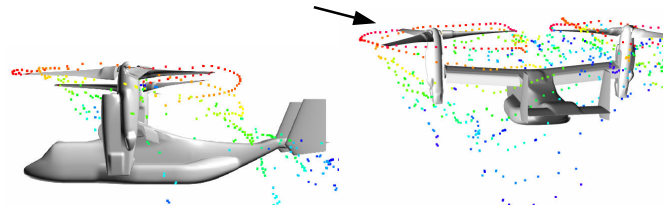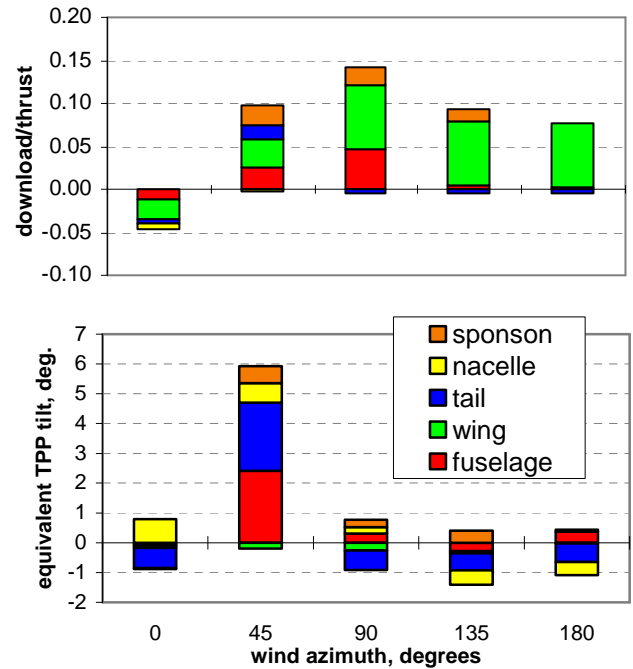
azimuth, although with significantly reduced magnitude and consequences compared with the quartering headwind.

PUWSS is known to be due to the rotor wake impinging on the empennage. CFD flow visualizations confirm this as seen in Figure 12. In this image, extracted from a time-dependent OVERFLOW-D animation, particles released from the upwind (left) blade tips impact on the aft fuselage and empennage. Particles are colored by release time. Additionally, a breakdown of the OVERFLOW-D time-averaged DL/T and TPP tilt by airframe component in Figure 13 indicates that the majority of the pitch-up does indeed come from the tail as well as the fuselage.

OVERFLOW-D instantaneous (but representative) pressure forces in the download direction, shown in Figure 14 as a function of wind azimuth, are further indication of the decreased lift or increased download on the tail and aft cargo ramp. Blue coloring on the configuration indicates upload while red indicates download. Comparing the head

7

and sidewind cases with the 45° quartering wind, reduced upload on the tail upper surface and increased download on the tail lower surface and fuselage underside translate into the pitch-up. From the pressures it is seen that the upwind (left) vertical tail blocks the wake from hitting the horizontal tail behind it.

Figure 15 shows the Rot3DC pressures on the bottom of the V-22 as a function of wind speed for the critical 45° wind azimuth. As a function of wind speed, pressure forces on the upper surface appear to have less of an effect on the pitching moment than the bottom surface and are not shown. When the freestream velocity is 15 knots, a region of low pressure (blue) is evident near the front of the left sponson, with the wind coming from the top left as indicated. As wind speed increases the low pressure region grows in size and moves toward the tail. When the freestream velocity is 45 knots, the low pressure region envelops the lower surface of the tail. This suction on the tail directly contributes to the pitch-up as wind speed increases beyond 25 knots.

In an attempt to reduce the exposed area of the horizontal tail and increase its lift, the elevator was deflected 60 degrees down as shown in Figure 16. The nose up moment is reduced by 25% or 1.5° of equivalent TPP tilt. This result is for the reduced tip speed, $M_{tip} = 0.625$, using OVERFLOW-D. The reduction in pitching moment comes solely from the tail contribution. It is not known if this is a viable operational option for the V-22, which has a current 20° maximum elevator travel.

Increasing Power in Sideward Flight

Increased power requirements in sideward flight were revealed in V-22 EMD critical azimuth testing. It is seen in Figure 5 that power required (mast torque) to hover in sidewinds is 10-20% higher than no/low-wind hover. In constant high wind conditions the power required to hover increases drastically (up to 80%) as the wind direction moves from a headwind towards a sidewind. CFD clearly shows this to be an adverse rotor-fuselage interaction due to an increase in airframe download. There may also be adverse rotor-on-rotor interference.

The increase in power required in sideward flight can be directly correlated with an increase in download. Download over thrust trends in Figures 10 and 11 as a function of wind azimuth are clear, and Rot3DC and OVERFLOW-D are in good agreement on download predictions. All wind speeds indicate increasing DL/T as wind azimuth is increased up to the sidewind condition. Further increasing to 135° azimuth results in values similar to 45°. From 135° to 180° the DL/T is roughly constant. Although both CFD calculations predict a download in a tailwind compared with the upload in a headwind, flight test data indicate the power required in these two conditions is approximately the same (Figure 6). These conditions may
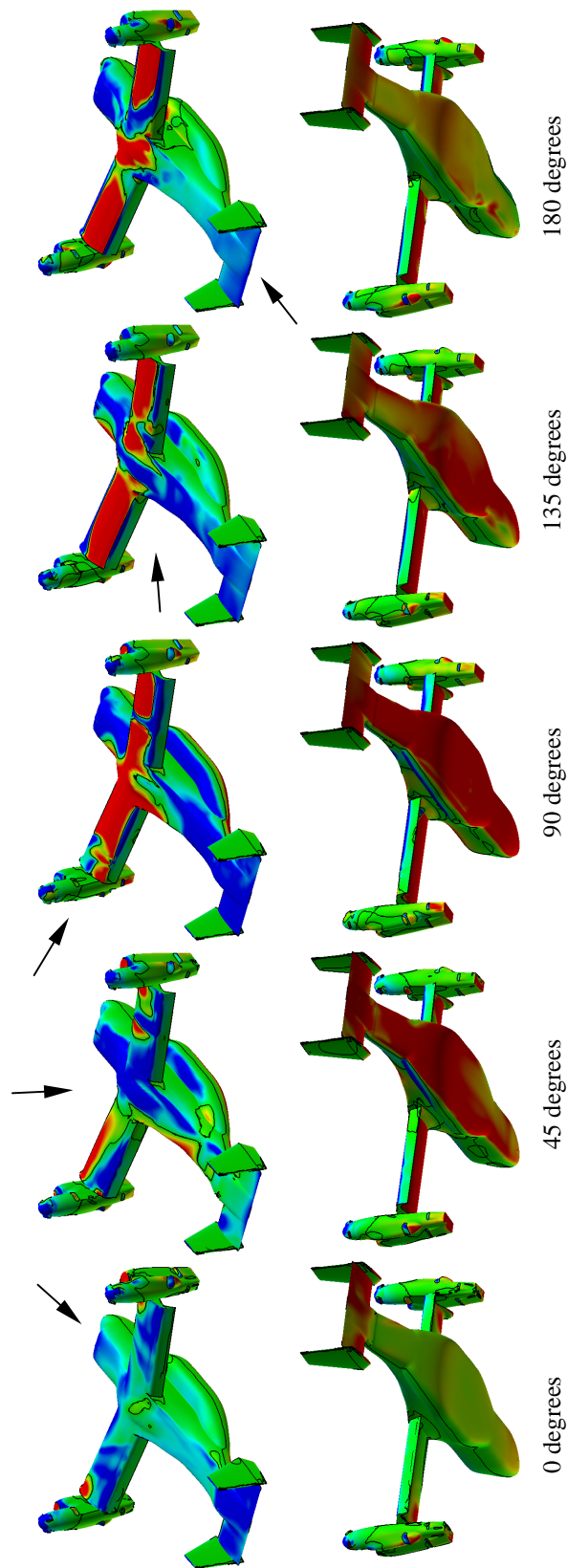

Figure 14 OVERFLOW-D instantaneous pressure force in download direction as a function of wind azimuth, 35 knot wind, blue – upload, red – download, black line – zero contour, arrow – wind direction.

0 degrees 45 degrees 90 degrees 135 degrees 180 degrees
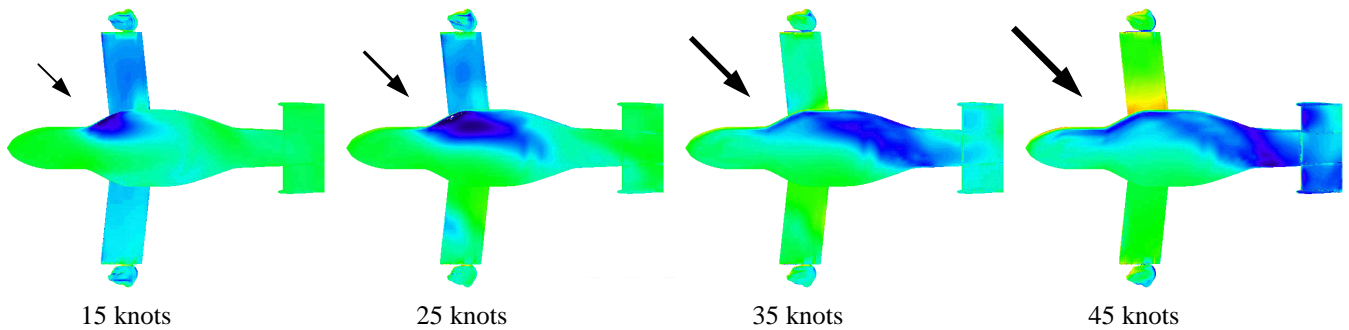
| 15 knots | 25 knots | 35 knots | 45 knots |

Figure 15 Rot3DC time-averaged pressure as a function of wind speed, 45° wind azimuth, bottom view, blue – low, arrow – wind direction scaled by wind speed.

be especially sensitive to fuselage pitch attitude, which is not taken into account in the CFD.

Rot3DC calculations confirm that the increasing power in sideward flight phenomenon is exacerbated by increased wind speed (Figure 10). As the freestream velocity is increased, both the DL/T magnitude at 90° and the slope from 0° to 90° azimuth increase. For a wind speed of 35 knots with intermediate data points, the DL/T sharply increases between a wind azimuth of 30 and 60 degrees. Similar trends might be expected for 45 knots. Dimensional download at 90° azimuth is increased by 25% as the hover tip Mach number is increased from 0.625 to 0.736 in OVERFLOW-D. Nondimensionally, the crosswind DL/T is reduced by 10% for the higher rotor RPM.

Based on the component breakdown in Figure 13 and the pressure forces in the download direction in Figure 14, it is seen that in a 35-knot headwind all parts of the airframe are lifting. As the wind passes through 45° the upload on the wing upper surface and fuselage aft upper surface have changed to a download. At 90° the download due to the rotor wake on the wing upper surface is now significant. The flat bottom lower surface of the fuselage also has a large influence, even more noticeable for reduced hover tip Mach number (not shown). The suction on this surface steadily increases as the wind direction approaches 90°. While the download value at 135° is similar to 45°, in

Figure 16 OVERFLOW-D effect of elevator deflection on PUWSS, M_{tip} = 0.625.

comparison, there is an increased contribution from the wing due to the rotor wake impinging on the wing upper surface and separation off the flap. There is a smaller contribution from the fuselage ramp.

With a tailwind, wing download remains larger than with a headwind. This is due to the wake and tilt rotor fountain remaining over the wing when rotor swirl velocities are in opposition to the oncoming flow. This effect is evident in Figure 17, which shows OVERFLOW-D velocity magnitude contours in a streamwise plane through the aircraft CG and a centerline plane for both 35-knot head and tailwinds. For this reason the tailwind case also shows significant unsteadiness in rotor and airframe forces compared with a headwind (Figures 7 and 8).

Rot3DC average rotor Figure of Merit, normalized by the headwind value, is shown in Figure 18 as a function of wind azimuth and speed. Although Figure of Merit is a measure of no-wind hover performance, it provides insights into the effect of sideslip on the rotor performance. This plot indicates noticeably reduced rotor efficiency for a 90° wind azimuth. Trends with wind speed are consistent and show reduced efficiency for the sidewind condition with increasing wind speed. The curves are relatively symmetric about the sidewind case. For the 45-knot case, individual upwind and downwind rotor performance is also shown. The upwind rotor performance improves slightly as the wind azimuth approaches 90° because the upwind rotor sees reduced interference from the downwind rotor. The downwind rotor suffers significantly, operating in the induced downwash from the upwind rotor wake. OVERFLOW-D calculated rotor performance remains relatively constant or slightly increasing as a function of wind azimuth for constant wind speed (e.g., Figure 7) and does not indicate this trend for the downwind rotor.

As expected there is a significant increase in side force on the fuselage as the wind approaches 90° (Figure 8). The side force divided by thrust in a 35-knot direct crosswind is 0.105. This requires an equivalent 6° roll attitude into the wind to counteract.

The increasing power in sideward flight phenomenon was not identified on the XV-15, possibly due to a more
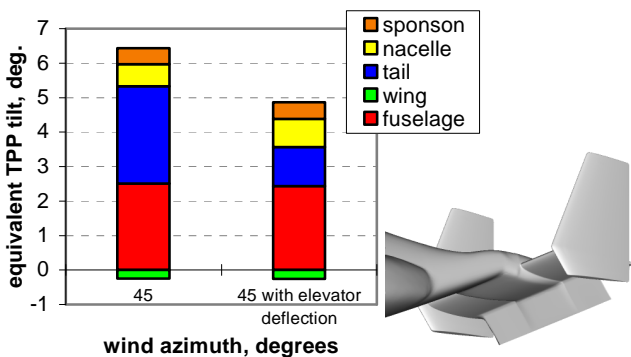
streamwise

centerline

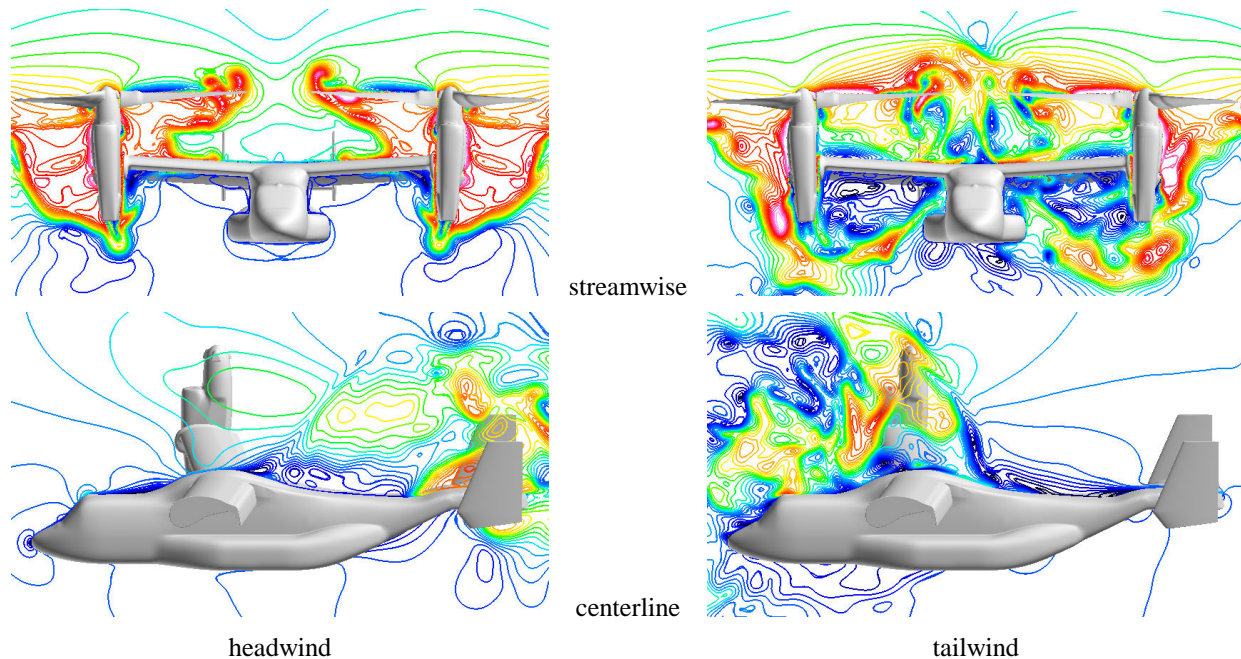headwind   tailwind

Figure 17   OVERFLOW-D velocity magnitude contours in a streamwise plane at the aircraft CG and a centerline plane, 35-knot head and tailwinds, blue – low, red – high.

rounded fuselage shape. It is noted that for the V-22 the unpowered airframe shows a trend of increased download with sidewind (Figure 11), but this phenomena is magnified by the rotor downwash impinging on the wing upper surface and causing additional suction on the fuselage lower surface. The consequences of this rotor-fuselage interaction are significant. Developing an experimental model that can be turned through 180° of sideslip without interfering with the fuselage flowfield is difficult. CFD calculations have shown this to be a tractable problem, implying that future fuselage shapes can be investigated provided rotor interactions are included. Adverse rotor-on-rotor interference is not supported by the XV-15 data, and CFD results are contradictory. In flight the roll attitude of the

Figure 18   Rot3DC normalized Figure of Merit as a function of wind azimuth and speed.

aircraft may reduce the sidewind rotor-on-rotor interference due to separation of the wakes.

Forward/Rearward Flight

In forward and rearward flight (0°/180° azimuth) some interesting aeromechanics phenomena occur. Around a 25-knot wind speed, the V-22 flight test power required to hover drops dramatically within 5 knots (Figure 6). Similar trends were seen on the XV-15 starting at 20 knots [3]. Wind tunnel tests by McVeigh [4] on a 0.15-scale V-22 with 0.71 hover tip Mach number show a more gradual reduction in DL/T starting around 13 knots. The particular speed is a function of the fuselage pitch attitude. For zero pitch attitude, the wind tunnel model airframe generates lift starting around 27 knots. Both flight test and wind tunnel experiment indicate at least a 10% increase in power required or DL/T above no-wind hover values just before the decrease. The reasons for the sharp reduction in flight test power required and precursory rise are not clear.

CFD predicted DL/T values are shown in Figure 19 as a function of normalized headwind speed. The wind speed is normalized by the hover induced velocity in order to account for the significant differences is rotor tip speed. For OVERFLOW-D a moderate decrease in DL/T is calculated starting around 20 knots. A substantial increase just before this download reduction is not predicted as in flight and wind tunnel test. OVERFLOW-D and Rot3DC predict similar initial DL/T values for low wind speeds. OVERFLOW-D shows a steepening trend at higher wind speeds, while Rot3DC results are more gradual. Wind
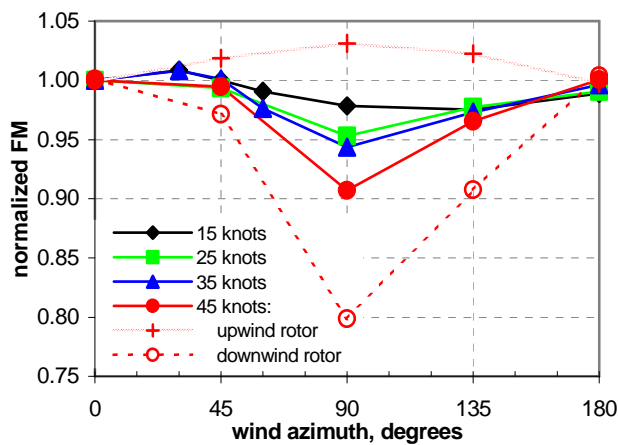
tunnel test data [4] are also plotted and show an intermediate trend. None of these DL/T slopes are as steep as the sharp reduction in flight test mast torque (Figure 6). Both CFD codes predict an upload generated by the airframe starting at 30 knots, in general agreement with wind tunnel and flight test data. It is suspected that the disagreement between Rot3DC and OVERFLOW-D in headwind conditions is related to the lack of geometric fidelity in Rot3DC. Head on, the V-22 presents a more streamlined shape compared with sideslip conditions, and the aerodynamics are more subtle.

The physical mechanism for the reduction in download is related to the wake being gradually convected past the wing. This is apparent when examining the CFD velocity flowfields generated by OVERFLOW-D in Figure 20. The plots depict the rotor wakes in a streamwise plane at the aircraft CG (through the rotor centers) and a spanwise plane at 55% wing semispan. The flowfields are generally laterally symmetric, except in hover [5]. The interaction of the rotor wake with the fuselage is shown. In up to 15-knot winds, the tilt rotor fountain is over the fuselage and the flow underneath the wing is recirculating, both creating significant download. Starting at 20 knots the rotor wake begins to be convected past the upper and lower surfaces of the wing. By 25 knots half the wing undersurface is in a clean flowfield. The airframe begins lifting at 30 knots. At 35 knots a large percentage of the upper and lower wing surfaces are undisturbed by the rotor wake except near the nacelle.

CFD-predicted power required normalized to the 15-knot headwind value is also shown in Figure 19 as dashed lines. Power required is calculated as the predicted rotor torque corresponding to a fixed gross weight ($C_W = C_T = 0.015$) plus an increment in power to compensate for the calculated download and estimated jet
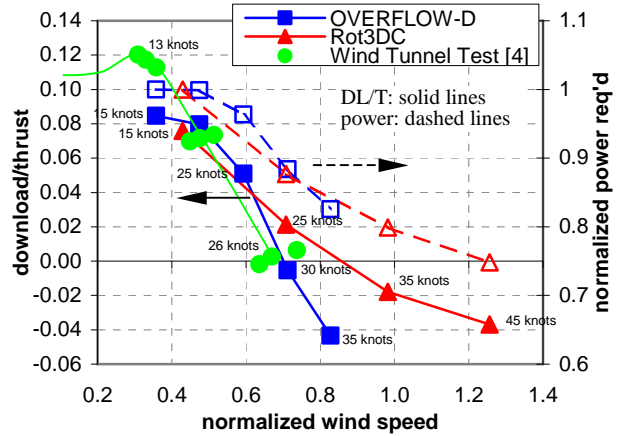

Figure 19 Rot3DC and OVERFLOW-D DL/T and normalized power required as a function of normalized headwind speed.

thrust ($\sim 0.025 C_W$). Power increments are calculated assuming constant Figure of Merit (FM) at each wind speed. Because FM is steadily increasing with wind speed, power required follows a gradual trend. No sharp drop in power is seen as with the flight test data. As depicted in the flow visualization, the wake moves across the wing steadily reducing download. Similarly, lift generated by the wing should increase at a rate proportional to the square of the wind speed with no abrupt increases.

Critical azimuth flight testing indicates that at the transition speed there is considerable lateral instability, perhaps generated by asymmetric shedding of the wake off the wing [1]. This power reduction phenomenon and overshoot precursor may, therefore, be a complex rotor-airframe interaction, possibly related to pitch attitude and nacelle tilt, which are not modeled in the CFD. However, understanding this phenomenon may assist ongoing download reduction efforts.
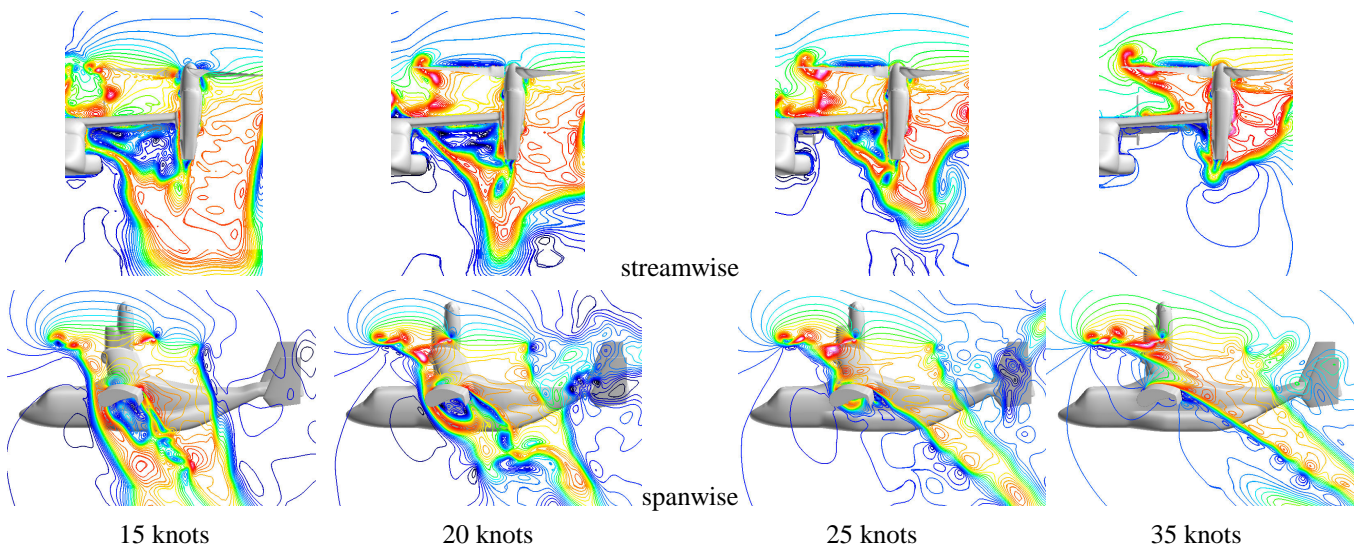

Figure 20 OVERFLOW-D velocity magnitude contours in a streamwise plane at the aircraft CG and a spanwise plane at 55% wing semispan as a function of headwind speed, blue – low, red – high.

CONCLUSIONS

Aeromechanics phenomena affecting the V-22 tilt rotor in low speed flight or while hovering in wind from varying azimuths have been investigated using computational fluid dynamics. Results have been compared with available wind tunnel and V-22 flight test data, although head-to-head comparisons were generally not possible. The following conclusions are made from the results presented:

- Pitch-up with sideslip (PUWSS) is caused by an adverse interaction of the rotor wake impinging on the aft fuselage and empennage. It is not present in rotor-off fuselage characteristics. Large down elevator deflections mitigate the phenomenon.

- Airframe pitch characteristics are in excellent agreement between CFD and flight test, with wind azimuth and speed trends correctly captured: maximum pitch-up at 45 degrees wind azimuth, increased severity with wind speed, and pitch-down in tailwinds.

- Increasing power in sideward flight is caused by significantly increased download on the wing upper surface and fuselage flat lower surface, exacerbated by increased wind speed. Rotor-on-rotor interference effects may exist, but CFD and flight test data (V-22, XV-15) are contradictory.

- For forward flight, a sharp reduction in power required in V-22 flight test at a particular headwind speed and a precursory overshoot are not captured by CFD. DL/T and power required are shown to present a more gradual trend with increasing wind speed.

OVERFLOW-D and Rot3DC offer complementary CFD capabilities to investigate aeromechanics phenomena. OVERFLOW-D obtains high-fidelity, turbulent, moving body computations at considerable cost, while Rot3DC uses lower geometric and physical fidelity, including a momentum source actuator disk, for fast turnaround on commodity computers. For low speed tilt rotor analyses, the following conclusions regarding code comparison are made:

- Download calculations as a function of wind azimuth are in excellent agreement between Rot3DC and OVERFLOW-D, except for headwind conditions, which are only in fair agreement. Pitch characteristics compare well.

- Rot3DC offers sufficient accuracy to determine airframe force and moment trends at a low cost. It would most likely be used for preliminary analysis and design. However, due to modeling fidelity, OVERFLOW-D solutions are probably required for detailed investigation of flowfield physics and more accurate airframe predictions.

Overall, CFD is an effective tool for predicting complex rotor-airframe interactions on new and current tilt rotor configurations in sideward flight for reduced risk in design and flight test. Complex aeromechanics phenomena can be best explained using a combination of airframe forces and moments, rotor performance, and detailed flowfield visualization.

ACKNOWLEDGEMENTS

REFERENCES

1. Klein, G., Roberts, B., and Seymour, C., "MV-22 Handling Qualities Flight Test Summary," American Helicopter Society 56th Annual Forum, Virginia Beach, VA, May, 2000.

2. McDonald, H. et al., "Tiltrotor Aeromechanics Phenomena: Report of Independent Assessment Panel – Final Report," November 2001.

3. Arrington, W.L., Kumpel, M., Marr, R.L., and McEntire, K.G., "XV-15 Tilt Rotor Research Aircraft Flight Test Data Report, Volume II of V: Performance and Handling Qualities," NASA CR 177406, June 1985.

4. McVeigh, M. A., Grauer, W. K., and Paisley, D. J., "Rotor/Airframe Interactions on Tiltrotor Aircraft," American Helicopter Society 44th Annual Forum, Washington, DC, June 1988.

5. Potsdam, M. A. and Strawn, R. C., "CFD Simulations of Tiltrotor Configurations in Hover," American Helicopter Society 58th Annual Forum, Montreal, Canada, June 2002.

6. Poling, D. R., Rosenstein, H, and Rajagopalan, R. G., "Use of a Navier-Stokes Code in Understanding Tiltrotor Flowfields in Hover," *Journal of the American Helicopter Society*, Vol. 43, No. 2, April 1998.

7. Meakin, R. L., "Unsteady Simulation of the Viscous Flow About a V-22 Rotor and Wing in Hover," AIAA

Paper 95-3463, Atmospheric Flight Mechanics Conference, Baltimore, MD, August 1995.

8. Tai, T.C. and Vorwald, J., "Simulation of V-22 Rotorcraft Hover Flowfield," AIAA Paper 93-4878, 1993 AIAA International Powered Lift Conference, Santa Clara, CA, December 1993.

9. Felker, F., Shinoda, R., Heffernan, R., and Sheehy, H., "Wing Force and Surface Pressure Data from a Hover Test of a 0.658-Scale V-22 Rotor and Wing," NASA Technical Memorandum 102244, February 1990.

10. Johnson, W., "Calculation of Tilt Rotor Aeroacoustic Model (TRAM DNW) Performance, Airloads, and Structural Loads," Proceedings of the American Helicopter Society Aeromechanics Specialists' Meeting, Atlanta, GA, November 2000.

11. Chan, W. M., Meakin, R. L., and Potsdam, M. A., "CHSSI Software for Geometrically Complex Unsteady Aerodynamic Applications," AIAA Paper 2001-0593, 39th Aerospace Sciences Meeting and Exhibit, Reno, NV, January 2001.

12. Rajagopalan, R. G., "A Procedure for Rotor Performance, Flow Field, and Interference: A Perspective," AIAA Paper 2000-0116, 38th AIAA Aerospace Sciences Meeting and Exhibit, Reno, NV, January, 2000.

13. Rajagopalan, R. G. and Lim C. K., "Laminar Flow Analysis of a Rotor in Hover," *Journal of the American Helicopter Society,* Vol. 36, No. 1, 1991.

14. Patankar S. V., "Numerical Heat Transfer and Fluid Flow," Hemisphere Publishing Corporation, New York, 1980.